J. Water Environ. Nanotechnol., 5(4): 369-377 Autumn 2020

ORIGINAL RESEARCH PAPER

Interaction of Crizotinib (as an anti-lung cancer drug) on Pure, Boron-Doped, and Carboxylated C60 Fullerene: Based on Density Functional Theory

Ashraf Sadat Ghasemi*, Mohammad Kia Kiani, Fatemeh Ravari

Chemistry Department, Payame Noor University, Tehran, Iran

Received: 2020-08-14 Accepted: 2020-09-20 Published: 2020-11-15

ABSTRACT

Notwithstanding the enormous benefits of crizotinib, as an anti-lung-cancer drug, severe toxicity as side effects are the main issues for this drug. In this research, the interaction of crizotinib over NH2 agent with C60 fullerene, boron-doped fullerene (C59B), and carboxylated fullerenes (C60COOH) using density functional theory at B3LYP/6-311G(d) theoretical level in the water solvent and gaseous phase were evaluated. Comparison of the drug-fullerenes complex in terms of structure, energy, and type of interaction was performed through optimization, frequency, natural bond orbital, and atoms in molecules calculations. The results indicated that the interaction of the drug with fullerenes due to the positive interaction energy and the unstable complexation could not be proper interaction between the drug and the nanoparticle. Binding between crizotinib and $C_{59}B$ is covalent, and the drug absorption is chemical. The interaction between crizotinib with $C_{60}COOH$ has been recognized as appropriate due to some properties such as higher solubility in water, relative stability, hydrogen bonding, and physical absorption of the drug. The result of this research could be counted as a promising strategy in order to reduce the toxicity and develop the anti-lung-cancer activity of crizotinib.

Keywords: *AIM, C60 Fullerene, Crizotinib, DFT, NBO*

How to cite this article

Ghasemi A. S., Kia Kiani M., Ravari F. Interaction of Crizotinib (as an anti-lung cancer drug) on Pure, Boron-Doped, and Carboxylated C60 Fullerene: Based on Density Functional Theory. J. Water Environ. Nanotechnol., 2020; 5(4): 369-377.
DOI: 10.22090/jwent.2020.04.007

INTRODUCTION

Crizotinib (CZT) under the brand name XALKORI® is an anti-cancer drug that prevents the growth and spread of cancer cells in the body [1]. CZT inhibits chemicals in order to block the growth of cancer-free cells that survive longer than normal cells. It is employed to treat certain types of non-small cell lung cancers that have spread to other parts of the body [2, 3]. The CZT is a tyrosine kinase inhibitor that inhibits the growth and spread of cancer cells. It neutralizes the effects of abnormal and carcinogenic proteins made by the anaplastic lymphoma kinase (ALK) disrupted gene [4]. In 2011, CZT was approved by the food and drug administration for this form of lung cancer [5].

The fullerenes are highly electronic and react efficiently to the nucleophiles. Also, C60 is the prototype cage-like structure. Fluorine carbon atoms can react with atoms and molecules without altering their stability and spherical structure. Researchers are keen to create new molecules by adding other molecules to the outer part of fluorine [6, 7]. Due to their unique properties, fullerenes have attracted much attention, which has made them attractive for a wide range of applications. Substitutional doping of different fullerene structures with different transition metals such as

* Corresponding Author Email: *ashraf.ghasemi@gmail.com*

nickel, ruthenium, chromium, zirconium, titanium, palladium, and molybdenum for electronic and non-linear optical applications was studied [8-11]. However, the low solubility of fullerenes in fluids limits the use of these substances as active pharmaceutical ingredients (API). However, its size, hydrophobia, three-dimensionality, and electronic properties prevent it from not being treated as a medicine and food emulsion [12-15]. For example, their spherical shape creates the ability and location of fullerenes molecules in hydrophobic solutions of enzymes or cells. Therefore, it could be said that the size, hydrophobic nature, three-dimensional structure, and electronic structure of fullerenes makes them attractive for pharmaceutical chemistry [16, 17]. In many studies, in order to improve the properties of fullerenes and nanotubes, atoms such as boron, silicon, sulfur, and zinc and … have been replaced by one or more carbon atoms of fullerenes or nanotubes, which these doped nanoparticles have been used in drug delivery [18-21]. Fullerene functionalization improves the properties of these nanoparticles, including increasing their solubility, as well as the use of these external association derivatives in pharmaceuticals. Therefore, functionalized fullerenes such as hydroxyl, carboxyl, and other functional groups have attracted much attention due to their capabilities in the field of material science, biochemistry, and biotechnology [22-29]. In this research, in order to compare the energy of the drug interaction in the water and gas phase, calculations were also performed in the gas phase. Hence, the optimal energy for a complex is considered that, firstly, it does not have chemical interactions and, secondly, does not have very weak intermolecular attractions.

METHODS

Structural and electronic properties and the interaction of CZT, fullerene C 60, boron-doped fullerenes, and the fullerene functionalized with carboxyl functional groups have been studied by the functional density theory method. All optimization calculations were performed by Gaussian 09 software developed by the Gaussian (United States of America). Software such as gauss view and AIM2000 were also used in order to draw molecules, analyze data, and draw diagrams. The theoretical level of B3LYP/6-311G (d) was used in the DFT method in the gas and water solvent phase. Comparison of drug-fullerenes complex, in terms of structure, energy, and type of interaction, has been done through optimization calculations, frequency, natural bond orbital (NBO), and atoms in molecules (AIM). A comparison was also made between relative energy, dipole moment, structural parameters, the highest employed molecular orbital (HOMO), and the lowest unoccupied molecular orbital (LUMO) in various complexes. The solvent effects of water on the primary molecules and the drug's interaction with fullerene were studied using the self-consistent reaction field (SCRF) in the polarizable continuum model (PCM).

The interaction energy of the drug is calculated by the following equation [22]:

$$E_{int} = E_{complex} - (E_{nano} + E_{CZT}) + E_{BSSE} \quad (1)$$

Where, E_{CZT} and $E_{complex}$ are the energy levels of CZT, and the energy level of the drug-fullerene complex, respectively. Also, E_{C60} is the representative of C60 fullerene, boron-doped fullerene (C59B), and carboxyl-functionalized fullerene (C60COOH). When calculations are performed for the complex system, the essential functions of both nuclei are effective in shaping the type of interaction, and therefore in the final energy, this issue must be taken into account. Therefore, the basis set superposition error (BSSE) was calculated and considered in the calculation of interaction energy [30].

In AIM theory, ρ(r) is described by a set of critical points (CP). At the critical point, the gradient vector of the electron density ∇ρ(r) is zero. Electron density (r) is one of the few scalar fields that could be used to represent critical points. Laplace electron density (r) is another of the most critical scalar fields. The two atoms interacting in the molecule form a critical point in the electron density called the BCP bonding critical point. The pair of gradients that start at one BCP and end at adjacent nuclei is called the Link path.

On the other hand, according to the following equation, Laplace of the electron density at any point in space balances between the potential energy density and the kinetic energy density [31]:

$$2G(r) + V(r) = \frac{1}{4}\nabla^2\rho(r) \quad (2)$$

G(r) is the density of electronic kinetic energy, which is always with power, and *V(r)* is the potential and numerical energy density with a negative sign [32]. Electronic density, which can be represented by the following presentation, could manage the density of the kinetic system and potential equally

[33].

$$H(r) = G(r) + V(r) \quad (3)$$

In the NBO method, a one-electron density matrix is used to define the shape of atomic orbitals in a molecular environment and to obtain molecular bonds (the electron density between atoms). The chemical potential μ is calculated from the following equation [34]:

$$\mu = \frac{E_{(HOMO)} + E_{(LUMO)}}{2} \quad (4)$$

The chemical hardness of the molecule ($\eta\eta$) could be calculated using Koopman's theory as follows [35]:

$$\eta = \frac{(IP - EA)}{2} \quad (5)$$

Which ionization potential (IP) are defined as IP = $-E_{(HOMO)}$ and the electron energy (EA) as EA = $-E_{(LUMO)}$. Therefore, the relevant equation is as follows [36]:

$$\eta = \frac{E_{LUMO} - E_{HOMO}}{2} \quad (6)$$

Chemical hardness is a resistance measurement of a chemical species to the change in electron arrangement, while the chemical potential is a measure of the system's tendency to lose electron clouds. In order to obtain more details, the electrophilicity index (ω) has been calculated. The degree of energy stability of the system is measured during the load transfer with its surroundings. A more significant value $\omega\omega$ indicates the strength of the structure [37]:

$$\omega = \frac{\mu^2}{2\eta} \quad (7)$$

The degree of softness is also related to the hardness values by the following equation [38]:

$$s = \frac{1}{2\eta} \quad (8)$$

Soft molecules have more reactivity and chemical activity than other molecules.

RESULTS AND DISCUSSION

Calculation of energy, dipole moment, and geometric structure

Using GaussView software, the initial structure of the drug CZT, C60 fullerene, boron-doped fullerene, and carboxyl-functionalized fullerenes were drawn. The molecules were then optimized using the Gaussian software at the B3LYP/6-31G(d) theory level. The amine group-administered CZT alongside each of the three fullerenes, and optimized drug interactions with this pure, boron-doped fullerene and carboxyl-activated group with B3LYP/6-311G(d) theory levels in gas and water phases were performed. The doped structures of the drug and the CZT-C60, CZT-C59B, and CZT-C60COOH complexes are shown in Fig. 1. Also, Table 1 shows the Gaussian output in terms of energy extracted from Harter in gas and water phases.

As could be seen from Table 1, the energy of all molecules in water is lower than that of the gas phase, which indicates that the molecules are more stable in the water phase. Also, the calculated values of interaction energies in complexes and dipole moment of the drug, C60 fullerene, and the complexes are shown in Table 2.

According to the data on the interaction energy in Table 2, the interaction between the drug and fullerenes in both gas and water phases is hot, indicating that drug uptake on fullerenes are not spontaneous and the CZT-C60 complex in both the gas and water phases are unstable. Drug uptake on boron-doped fullerenes and carboxyl-functionalized fullerenes are exothermic. The energy values of the interaction between the drug and the doped fullerene indicate a strong interaction that could indicate the covalent attraction between the boron atom from the doped fullerene and the nitrogen atom from the drug. The release of the drug is more critical than the adsorption on C60 fullerene. So, it appears that this interaction between the drug and the boron-doped fullerene (C59B) cannot be suitable for drug delivery. The interaction energy between the drug and the carboxyl-functionalized fullerene could indicate the presence of our attractions between vandalism and covalent, that is, within the range of hydrogen bonding, which could generally be appropriate in drug transfer with nanoparticles [39]. In all cases, for medicine, pure fullerene and boron-doped fullerene and carboxyl-functionalized fullerene, and the dipole moment complexes in the water phase are larger than the dipole moment in the gas phase. Between boron-fermented fullerenes and carboxyl-functionalized fullerenes, carboxyl-functionalized fullerenes have a larger dipole moment, indicating that their solubility in water,

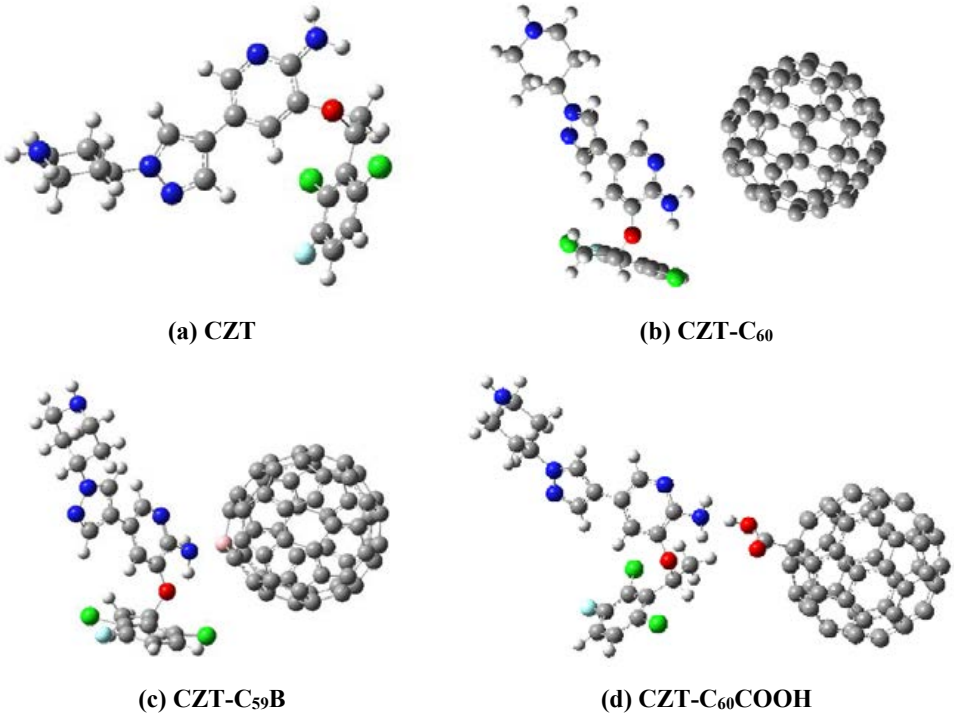

(a) CZT **(b) CZT-C_{60}**

(c) CZT-$C_{59}B$ **(d) CZT-$C_{60}COOH$**

Fig. 1. Optimized structure of CZT drug and complexes

Table 1. Gaussian output in terms of energy extracted from Harter

	CZT	C_{60}	$C_{59}B$	$C_{60}COOH$	CZT-C_{60}	CZT-$C_{59}B$	CZT-$C_{60}COOH$
Gas	-2182.656	-2286.174	-2272.903	-2475.311	-4468.830	-4455.590	-4657.986
Water	-2182.673	-2286.176	-2272.904	-2475.318	-4468.848	-4455.613	-4658.005

Table 2. Interaction energy (Kj/mole) and dipole moment (Debye)

	E_{int}		μ^0	
	Gas	Water	Gas	Water
CZT	-	-	2.037	2.418
C_{60}	-	-	0.000	0.000
$C_{59}B$	-	-	0.572	1.097
$C_{60}COOH$	-	-	1.342	1.808
CZT-C_{60}	4.747	6.681	1.718	2.402
CZT-$C_{59}B$	-59.504	-72.270	12.743	15.498
CZT-$C_{60}COOH$	-38.232	-25.644	6.517	6.993

as a polar solvent, is higher than that of pure and boron-doped fullerene. The CZT-C60 complex has less dipole moment and less water solubility than the single drug. If, for the other two complexes, the dipole moment is more massive than the single drug, and therefore their solubility in water is higher than the single drug. Also, the enormous dipole moment of the CZT-C59B complex is due to the more excellent stability of this complex in both phases, especially in the water phase.

The length changes of C-C bonds in pure C60 changed from 1.395 and 1.453 to 1.397 and 1.454

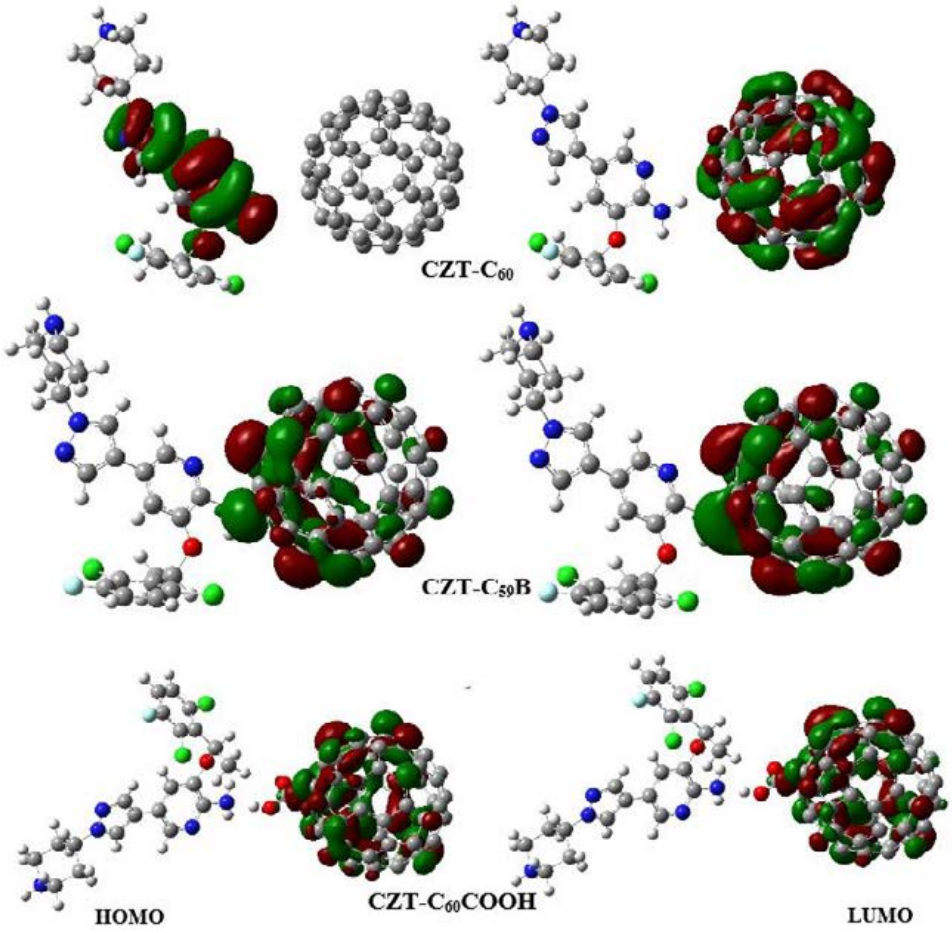

Fig. 2. HOMO and LUMO orbitals of complexes in the water phase

at the CZT-C60 complex, respectively. Besides, in the drug alone, the N23-H40 and N23-C12 bonds changed from 1.013 and 1.382 to 1.014 and 1.384 at the CZT-C60 complex, respectively. This indicates that the structure of the drug and C60 has not changed significantly. In the CZT-C59B complex, the B-C length bonds of pure nanoparticles changed from 1.526 and 1.548 to 1.598 and 1.619, respectively, and the N23-H40 and N23-C12 bonds from 1.013 and 1.382 in the drug alone to 1.024 and 1.459 in the complex, respectively. It was shown that the structure of the drug and C60 in this complex has changed to some extent. Also, in the CZT-C60COOH complex, the bond lengths of O-C and O-H bonds in pure nanoparticle changed from 1.210 and 0.977 to 1.216 and 1.020 in the complex, respectively, and the N23-H40 and N23-C12 bonds lengths changed from 1.013 and 1.382 in drug alone to 1.018 and 1.413 in the complex, respectively. The result showed that bond lengths change more than the CZT-C60 complex and less than the CZT-C59B complex. These results are in agreement with the order of the values of the interaction energies.

Chemical activity

The energies of the highest occupied molecular orbital and the lowest unoccupied molecular orbital, the gap energy, and general indicators indicating chemical activity for CZT, pure fullerene, and boron-doped fullerene, and carboxyl-functionalized fullerenes, and the corresponding complexes are given in Fig. 2 and Table 3. Fig. 2 shows the highest occupied orbital is on the drug molecule, and the lowest unoccupied orbital is on the fullerene nanoparticle at the CZT-C60 complex. Also, in the other two complexes, both HOMO and LUMO, are on the nanoparticle.

The chemical potential (μ) specifies the

Table 3. Values of the highest occupied molecular orbital energy (E_{HOMO}) and the lowest unoccupied molecular orbital energy (E_{LUMO}), gap energy (E_g), chemical potential (), chemical hardness (), electrophilicity index () and chemical softness (S) (eV) in the water phase

Complex	E_{HOMO}	E_{LUMO}	E_g	μ	η	ω	S
CZT	-5.402	-1.124	4.278	-3.263	2.139	2.489	0.234
C_{60}	-5.869	-3.108	2.761	-4.488	1.381	7.297	0.362
$C_{59}B$	-5.546	-4.235	1.311	-4.891	0.656	18.243	0.763
$C_{60}COOH$	-5.169	-3.684	1.485	-4.427	0.743	13.195	0.673
CZT-C_{60}	-5.263	-3.127	2.136	-4.195	1.068	8.239	0.468
CZT-$C_{59}B$	-4.859	-3.368	1.491	-4.114	0.746	11.349	0.671
CZT-$C_{60}COOH$	-5.129	-3.639	1.490	-4.384	0.745	12.899	0.671

Table 4. Bonding critical points (BCP) parameters in AIM calculations, electronic density (), electronic density laplacian (), electron kinetic energy density (), electron potential energy density () and total electron energy density () in the water phase

Complexes	Drug…Nanoparticle	ρ_{BCP}	$\nabla^2\rho_{BCP}$	G_{BCP}	V_{BCP}	H_{BCP}
CZT-$C_{59}B$	N83…B60	0.11128	0.31121	0.15337	-0.22893	-0.07556
	Cl84…C12	0.00238	0.00726	0.00137	-0.00093	0.00043
CZT-$C_{60}COOH$	N87…H64	0.05337	0.11986	0.03594	-0.04192	-0.00598
	H99…O63	0.00491	0.01809	0.00365	-0.00279	0.00086

direction of the charge transfer between two molecules. The transfer of electrons from a molecule with a higher chemical potential to a molecule with a lower chemical potential occurs. According to Table 3, the chemical potential of the drug is higher than that of all three fullerenes, indicating that the transfer of electrons in all three related complexes takes place from the drug to the fullerene. Gap energy is a quantity that determines the kinetic stability of a molecule. According to Table (3), Fullerene C59B has a higher polarity with lower gap energy and higher softness. Also, the considerable softness could indicate that pure fullerenes are more accessible to accept electrons than boron-doped fullerenes and other studied carboxyl-functionalized fullerenes. The larger C60 fullerene's gap energy gauge shows more stability and less willingness to interact.

For systems that have an individual electron, a separate orbital electron is defined for each electron [40, 41], and in Gaussian, the occupied and unoccupied orbital energy is different for the alpha and beta electrons. In the two drug complexes with doped and carboxyl-functionalized fullerenes, there is an individual electron, and we compare the gap energy between the two. The gap energy and its equivalent hardness in the CZT-C59B complex are slightly larger than the CZT-C60COOH complex, which indicates that it is stable.

Atoms in molecules analysis

Various parameters of the critical points of the bonds between the atoms of the drug CZT and pure fullerenes, the doped fullerenes, and the functionalized fullerenes, such as the electron density and the electron density Laplace, were used to study the type and strength of the bond. The data for the AIM software calculations are given in Table 4. The total electron energy density (HBCP) (electronic Hamiltonian) is also obtained from the sum of the electron potential energy density (VBCP) and the kinetic energy density (GBCP).

According to Table 4, the highest electron density of the critical point between the nitrogen atom (N83) of the drug and the boron atom (B60) of the doped fullerene, which indicates more accumulation of charge in the bond, and according to its amount and more significant amounts of laplacian, the electron density, and negativity of the total energy density indicate a covalent bond, which is in agreement with the corresponding energy of the complex formation interaction.

For hydrogen bonding (ρ_{BCP}), they are between 0.04-0.02 and $\nabla^2\rho_{BCP}$ 0.02-0.15, and relatively high values of density and positive $\nabla^2\rho_{BCP}$ and negative H_{BCP} values indicate that hydrogen interactions are covalent [42]. According to Table (4), the values of electron density and Laplace of electron density and negative total energy density, the critical point between the nitrogen atom of the drug (N87) and the hydrogen atom of the carboxyl group (H64) of the functionalized nanoparticle, indicate a hydrogen bond of quasi-quantum nature. The Cl84…C12 and H99…O63 bonds, in the CZT-

(a) CZT-$C_{59}B$

(b) CZT-$C_{60}COOH$

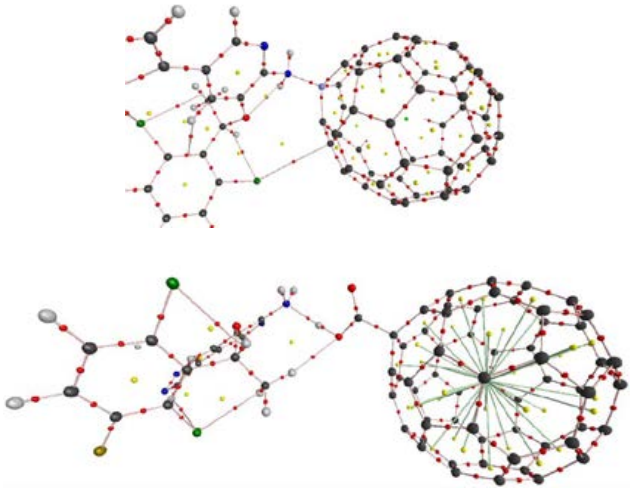

Fig. 3. Critical bonding points in (a) CZT-C59B and (b) CZT-C60COOH complexes

Table 5. The computed stabilization energy ($E^{(2)}$, Kcal/mole) of electron donor-acceptor complexes in the water phase.

Complexes	Donor → Acceptor	$E^{(2)}$
CZT-$C_{59}B$	$LP^*(1)C29 \rightarrow BD^*(1)B60 - N83$	3.85
CZT-$C_{60}COOH$	$LP(1)N87 \rightarrow LP^*(1)H64$	30.32

Table 6. Partial load values for atoms involved before and after drug interaction with carboxyl-functionalized fullerenes in the CZT-C60COOH complex in the water phase.

Atom No.	CZT-C60COOH	Drug (CZT)	C60COOH
C61	0.451	-	0.451
O62	-0.314	-	-0.299
O63	-0.364	-	-0.350
H64	0.259	-	0.262
C76	0.181	0.367	-
N87	-0.445	-0.845	-
H104	0.217	0.418	-
H105	0.218	0.420	-

C59B and CZT-C60COOH complexes, respectively, are of the Van der Waals attraction type shown in Fig. 3. Therefore, Fig. 3 shows the critical junctions between the drug and fullerene C60 in the CZT-C59B and CZT-C60COOH complexes.

Natural bond orbital analysis

Natural bond orbital (NBO) analysis is considered a useful tool for investigating the intermolecular interactions. The larger the $E^{(2)}$, the stronger the interaction between the donor electron (base Lewis) and the receiving electron (Lewis acid) [34]. The relevant results and load transfer of CZT-C59B and CZT-C60COOH complexes are given in Table 5.

According to Table 5, it is clear that the estimated values of the second-order energy disorder ($E^{(2)}$) for the interaction between CZT and fullerene C60COOH are very high, as well as the high tendency of electronic density by CZT to fullerene C60COOH. That is in line with the results of calculating the chemical potential. Also, Table 6 shows the result of partial loads of drug and fullerenes atoms in various types of interaction

in the C60COOH, CZT, and CZT-C60COOH complex.

It will be more stable for a complex that has more negative interaction energy. In the relevant complex, the hydrogen atom number 64 shows a less positive charge than when it is alone in fullerene. Furthermore, the nitrogen atom No. 87 shows a lower negative charge than when it is in the drug only before the interaction, which is expected due to the direction of charge transfer. The results indicate that the load distribution has changed during the attraction process.

CONCLUSIONS

Crizotinib, as an anti-lung-cancer drug, has substantial benefits in cancer therapy, but severe toxicity as side effects is the main problem for it. In this research, the interaction of crizotinib over NH2 agent with C60 fullerene, boron-doped fullerene (C59B), and carboxylated fullerenes (C60COOH) using density functional theory at B3LYP/6-311G(d) theoretical level in the gaseous phase and the water solvent were evaluated. Based on the information on optimization energies, data on chemical descriptors, and investigation of atoms in the molecules theory and natural bond orbital theory in the study of the interaction of CZT from the NH_2 group with C60 fullerene, C59B, and C60COOH has been concluded that drug interactions with fullerenes cannot be a functional interaction between drugs and fullerenes due to the positive energy of the interactions and the instability of the resulting complex. By calculating the frequency, the first frequency was real (positive), and Nimag was zero. Also, due to the high energy and atomic theory data in the molecule, it has been determined that the bond between CZT and C59B is covalent, and the drug uptake on this fullerene is chemical. Therefore, it is thought that drug release will not be done well. For this purpose, this interaction and its resulting complex have been misdiagnosed. However, the interaction between CZT with C60COOH has been identified due to some properties such as good solubility in the water phase, excellent stability in energy efficiency and hydrogen bonding, and physical absorption of the drug with fullerene in AIM and NBO evaluation. The result of this research could be counted as a promising strategy in order to reduce the toxicity and develop the anti-lung-cancer activity of crizotinib.

CONFLICT OF INTERESTS

The authors declare that there are no conflicts of interest regarding the publication of this manuscript.

REFERENCES

1. Lin C, Shi X, Yang S, Zhao J, He Q, Jin Y, et al. Comparison of ALK detection by FISH, IHC and NGS to predict benefit from crizotinib in advanced non-small-cell lung cancer. Lung Cancer. 2019;131:62-8.
2. Liu, P., et al., *Crizotinib-induced immunogenic cell death in non-small cell lung cancer.* Nature communications, 2019. **10**(1): p. 1-17.
3. Liu Z, Jiang L, Li Y, Xie B, Xie J, Wang Z, et al. Cyclosporine a Sensitizes Lung Cancer Cells to Crizotinib Through Inhibition of the Ca2 /Calcineurin/Erk Pathway. SSRN Electronic Journal. 2018.
4. Zhang C, Li S-l, Nie Q, Dong S, Shao Y, Yang X-n, et al. Neoadjuvant Crizotinib in Resectable Locally Advanced Non–Small Cell Lung Cancer with ALK Rearrangement. Journal of Thoracic Oncology. 2019;14(4):726-31.
5. Su, Y., et al., *Distribution of ALK fusion variants and correlation with clinical outcomes in Chinese patients with non-small cell lung cancer treated with crizotinib.* Targeted oncology, 2019. **14**(2): p. 159-168.
6. Tan Z, Ni K, Chen G, Zeng W, Tao Z, Ikram M, et al. Incorporating Pyrrolic and Pyridinic Nitrogen into a Porous Carbon made from C60Molecules to Obtain Superior Energy Storage. Advanced Materials. 2016;29(8):1603414.
7. Ghasemi AS, Ashrafi F, Babanejad SA, Elyasi A. Study of the Physicochemical Properties of Anti-Cancer Drug Gemcitabine on the Surface of Al Doped C60 and C70 Fullerenes: A DFT Computation. Journal of Structural Chemistry. 2019;60(1):13-9.
8. Rad AS, Aghaei SM, Aali E, Peyravi M. Study on the electronic structure of Cr- and Ni-doped fullerenes upon adsorption of adenine: A comprehensive DFT calculation. Diamond and Related Materials. 2017;77:116-21.
9. Rad AS, Aghaei SM, Aali E, Peyravi M, Jahanshahi M. Application of chromium-doped fullerene as a carrier for thymine and uracil nucleotides: Comprehensive density functional theory calculations. Applied Organometallic Chemistry. 2017;32(2).
10. Shokuhi Rad A, Ayub K. Substitutional doping of zirconium-, molybdenum-, ruthenium-, and palladium: An effective method to improve nonlinear optical and electronic property of C20 fullerene. Computational and Theoretical Chemistry. 2017;1121:68-75.
11. Rad AS, Ayub K. Nonlinear optical and electronic properties of Cr-, Ni-, and Ti- substituted C 20 fullerenes: A quantum-chemical study. Materials Research Bulletin. 2018;97:399-404.
12. Kazemeini, H., A. Azizian, and M.H. Shahavi, *Effect of Chitosan Nano-Gel/Emulsion Containing Bunium Persicum Essential Oil and Nisin as an Edible Biodegradable Coating on Escherichia Coli O157:H7 in Rainbow Trout Fillet.* Journal of Water and Environmental Nanotechnology, 2019. **4**(4): p. 343-349.
13. Shahavi MH, Hosseini M, Jahanshahi M, Meyer RL, Darzi GN. Clove oil nanoemulsion as an effective antibacterial

agent: Taguchi optimization method. Desalination and Water Treatment. 2015;57(39):18379-90.
14. Azizkhani M, Jafari Kiasari F, Tooryan F, Shahavi MH, Partovi R. Preparation and evaluation of food-grade nanoemulsion of tarragon (Artemisia dracunculus L.) essential oil: antioxidant and antibacterial properties. Journal of Food Science and Technology. 2020.
15. Shahavi MH, Hosseini M, Jahanshahi M, Meyer RL, Darzi GN. Evaluation of critical parameters for preparation of stable clove oil nanoemulsion. Arabian Journal of Chemistry. 2019;12(8):3225-30.
16. Dumpis MA, Prokopenko VM, Litasova EV, Arutyunyan AV, Piotrovskii LB. Antioxidant Properties of Fullerene C60/Dihydroquercetin Composites. Pharmaceutical Chemistry Journal. 2018;51(10):881-3.
17. Jahanshahi M, Najafpour G, Ebrahimpour M, Hajizadeh S, Shahavi MH. Evaluation of hydrodynamic parameters of fluidized bed adsorption on purification of nano-bioproducts. physica status solidi (c). 2009;6(10):2199-206.
18. Ghasemi, A.S., et al., *Studying physicochemical characteristics of Flutamide adsorption on the Zn doped SWCNT (5, 5), using DFT and MO calculations.* Eurasian Chemical Communications, 2020. **2**(1): p. 138-149.
19. Ghasemi AS, Mashhadban F, Ravari F. A DFT study of penicillamine adsorption over pure and Al-doped C60 fullerene. Adsorption. 2018;24(5):471-80.
20. Rad AS, Samipour V, Movaghgharnezhad S, Mirabi A, Shahavi MH, Moghadas BK. X12N12 (X = Al, B) clusters for protection of vitamin C; molecular modeling investigation. Surfaces and Interfaces. 2019;15:30-7.
21. Hamed Mashhadzadeh A, Fathalian M, Ghorbanzadeh Ahangari M, Shahavi MH. DFT study of Ni, Cu, Cd and Ag heavy metal atom adsorption onto the surface of the zinc-oxide nanotube and zinc-oxide graphene-like structure. Materials Chemistry and Physics. 2018;220:366-73.
22. Sabirov DS, Terentyev AO, Cataldo F. Bisadducts of the C 60 and C 70 fullerenes with anthracene: Isomerism and DFT estimation of stability and polarizability. Computational and Theoretical Chemistry. 2016;1081:44-8.
23. Ebrahimpour, M., et al., *Nanotechnology in Process Biotechnology: Recovery and Purification of Nanoparticulate Bioproducts Using Expanded Bed Adsorption.* Dynamic Biochemistry, Process Biotechnology and Molecular Biology, 2009. **3**(2): p. 57-60.
24. Pérez Quiñones, J., et al., *Novel Brassinosteroid-Modified Polyethylene Glycol Micelles for Controlled Release of Agrochemicals.* Journal of agricultural and food chemistry, 2018. **66**(7): p. 1612-1619.
25. Jahanshahi, M. and M.H. Shahavi, *Advanced Downstream Processing in Biotechnology*, in *Biochemical Engineering and Biotechnology*, G. Najafpour Darzi, Editor. 2015, Elsevier. p. 495-526.
26. Shahavi, M.H., et al., *Expanded bed adsorption of biomolecules by NBG contactor: Experimental and mathematical investigation.* World Applied Sciences Journal, 2011. **13**(2): p. 181-187.
27. Mofidian, R., et al., *Generation Process and Performance Evaluation of Engineered Microsphere Agarose Adsorbent for Application in Fluidized-bed Systems.* International Journal of Engineering, 2020. **33**(8): p. 1450-1458.
28. Mofidian R, Barati A, Jahanshahi M, Shahavi MH. Fabrication of novel agarose–nickel bilayer composite for purification of protein nanoparticles in expanded bed adsorption column. Chemical Engineering Research and Design. 2020;159:291-9.
29. Mofidian R, Barati A, Jahanshahi M, Shahavi MH. Optimization on thermal treatment synthesis of lactoferrin nanoparticles via Taguchi design method. SN Applied Sciences. 2019;1(11).
30. Bakó I, Mayer I, Hamza A, Pusztai L. Two- and three-body, and relaxation energy terms in water clusters: Application of the hierarchical BSSE corrected decomposition scheme. Journal of Molecular Liquids. 2019;285:171-7.
31. Alizadeh M, Hosseinzadeh K, Shahavi MH, Ganji DD. Solidification acceleration in a triplex-tube latent heat thermal energy storage system using V-shaped fin and nano-enhanced phase change material. Applied Thermal Engineering. 2019;163:114436.
32. Mortazavifar A, Raissi H. Theoretical Prediction of Adsorption Properties of Carmustine Drug on Various Sites of the Outer Surface of the Single-Walled Boron Nitride Nanotube and Investigation of Urea Effect on Drug Delivery by DFT and MD. Journal of Cluster Science. 2017;29(1):93-9.
33. Afshar M, Emami FS, Darabi A, Hemati M. Electronic structures and magnetic properties of 3d magnetic atoms adsorbed on olympicene molecule: A density functional theory study. Materials Chemistry and Physics. 2017;199:471-6.
34. Shukla S, Srivastava A, Kumar P, Tandon P, Maurya R, Singh RB. Vibrational spectroscopic, NBO, AIM, and multiwfn study of tectorigenin: A DFT approach. Journal of Molecular Structure. 2020;1217:128443.
35. Jalali Sarvestani, M.R. and R. Ahmadi, *Investigating the Influence of Doping Graphene with Silicon and Germanium on the Adsorption of Silver (I).* Journal of Water and Environmental Nanotechnology, 2019. **4**(1): p. 48-59.
36. Abbasi, A., *The adsorption of sulfur dioxide and ozone molecules on boron nitride nanotubes: A DFT study.* Journal of Water and Environmental Nanotechnology, 2019. **4**(2): p. 147-156.
37. Arjmandi, M., et al., *Study of Adsorption of H2 and CO2 on Distorted Structure of MOF-5 Framework; A Comprehensive DFT Study.* Journal of Water and Environmental Nanotechnology, 2018. **3**(1): p. 70-80.
38. Mahdavian, L., *Calculation Study of Conversion Nitrate Ions to N2 and O2 by Zinc Oxide Nano-Cage (Zn12O12-NC).* Journal of Water and Environmental Nanotechnology, 2019. **4**(2): p. 167-173.
39. Niksefat Abatari M, Sarmasti Emami MR, Jahanshahi M, Shahavi MH. Superporous pellicular κ-Carrageenan–Nickel composite beads; morphological, physical and hydrodynamics evaluation for expanded bed adsorption application. Chemical Engineering Research and Design. 2017;125:291-305.
40. Hosseini M, Shahavi MH. Electrostatic Enhancement of Coalescence of Oil Droplets (in Nanometer Scale) in Water Emulsion. Chinese Journal of Chemical Engineering. 2012;20(4):654-8.
41. Hosseini, M., M.H. Shahavi, and A. Yakhkeshi, *AC & DC-currents for separation of nanoparticles by external electric field.* Asian Journal of Chemistry, 2012. **24**(1): p. 181-184.
42. Hammami F, Ghalla H, Nasr S. Intermolecular hydrogen bonds in urea–water complexes: DFT, NBO, and AIM analysis. Computational and Theoretical Chemistry. 2015;1070:40-7.